Biosensors and Bioelectronics 26 (2011) 3887–3893

Contents lists available at ScienceDirect

Biosensors and Bioelectronics

journal homepage: www.elsevier.com/locate/bios

A electrogenerated chemiluminescence biosensor for Ramos cancer cell using DNA encapsulated $Ru(bpy)_3Cl_2$ as signal probe

Xu Hun [a,b,*], Huaicheng Chen [a,b], Wei Wang [a,b,*]

[a] State Key Laboratory Base of Eco-chemical Engineering, China
[b] College of Chemistry and Molecular Engineering, Qingdao University of Science and Technology, Qingdao 266042, China

ARTICLE INFO

Article history:
Received 10 January 2011
Received in revised form 1 March 2011
Accepted 1 March 2011
Available online 8 March 2011

Keywords:
Electrogenerated chemiluminescence
$Ru(bpy)_3Cl_2$
Biosensor
Ramos cell

ABSTRACT

A label-free sensing technology for detection of Ramos cell was developed based on a signal probe $Ru(bpy)_3Cl_2$ (Ru) encapsulated by DNA. Gold electrode or magnetic bead as the sensing surface was firstly modified with long-strand DNA with five repeating units. Then two kinds of short-strand DNA are grafted onto the long-strand DNA to form DNA strands A and B (L-A and L-B) through the hybridization, respectively. The addition of aptamer initiates hybridization of L-A and L-B with the aptamer sequence. As the hybridization proceeds, the four kinds of DNA would finally transform into a three-dimensional network structure and the signal probe Ru was encapsulated by DNA simultaneously. When Ramos cells are introduced to interact with the aptamer, the signal probe is released. In order to confirm the generality of this method the ferrocenecarboxylic acid and luminol selected as a signal probe mode were also tested. The Ru used as a signal probe for electrogenerated chemiluminescence (ECL) detection was detailedly studied. With this ECL biosensor, detection limit as low as 58 cells/mL was achieved for Ramos cell. The biosensor also exhibited excellent sensitivity and selectivity.

1. Introduction

Molecular recognition toward specific cells is a key issue for cancer diagnosis and therapy and also has recently attracted much attention. Traditionally, cancers are diagnosed mostly based on the morphology of tumor tissues or cells. However, these morphologic features are difficult to be used to carry out early cancer diagnosis or to evaluate the complex molecular alterations that lead to cancer progression (Espina et al., 2005; Shangguan et al., 2006). Although many methods based on molecular probes such as ligands and antibodies can recognize the unique molecular signatures of cancer cells, some of these methods have relatively profound label progress (Hun et al., 2008; Murray et al., 2010). In addition, ligands and antibodies are not always elevated in the early stages of cancer development, when therapy is most effective. A wide-scale cancer cell testing requires the development of easy-to-use, and inexpensive analytical methods.

Aptamers possess numerous attractive features, including low molecular weight, easy and reproducible synthesis, high binding affinity and molecular specificity (Shangguan et al., 2007; Yang et al., 2005) fast tissue penetration and low toxicity (Cerchia et al., 2002), tunability in binding affinity, and long-term stability (Jayasena, 1999). These advantages have made aptamers an excellent alternative as molecular probes for biomedical studies and clinical applications (Famulok et al., 2007; Mayer et al., 2007; Layzer and Sullenger, 2007). Now lots of aptamers have been produced. These aptamers not only can target peptides, proteins, DNA and RNA, but also viruses, parasites and bacteria (Famulok et al., 2007; Mayer et al., 2007; Layzer and Sullenger, 2007).

To achieve the goal of early diagnosis of cancer, it is essential to have cancer-specific biomarkers that can be recognized by molecular probes. With development of aptamer technology, a group of target cell-specific aptamers have been selected by SELEX. However, the reported methods for the cell detection based on the aptamer–cell interactions were almost fluorescent methods (Huang et al., 2009a,b; Zheng et al., 2009; Cheng et al., 2010). A fluorescent "signaling aptamer" possesses adequate transducing elements to generate physically detectable signals from the recognition events, thus designing fluorescence-signaling aptamers have become the focal point of several recent studies. Because DNA and RNA do not contain intrinsically fluorescent groups, aptamers must be modified with external fluorophores to provide opportunities for fluorescence-based sensing. However, even slight modifications on aptamers may lead to significant loss of their affinity and specificity, and fairly small fluorescence responses are usually obtained upon target binding; therefore, their detection sensitivity is relatively

* Corresponding authors at: State Key Laboratory Base of Eco-chemical Engineering, 53 Zhengzhou Road, Qingdao 266042, China and College of Chemistry and Molecular Engineering, Qingdao University of Science and Technology, 53 Zhengzhou Road, Qingdao 266042, China. Tel.: +86 53284022750; fax: +86 532 84022750.
E-mail addresses: hunxu@sohu.com, hunxudr@yahoo.cn (X. Hun), wangwei9612@126.com (W. Wang).

0956-5663/$ – see front matter © 2011 Elsevier B.V. All rights reserved.
doi:10.1016/j.bios.2011.03.004

low (Huang et al., 2009a,b; Zheng et al., 2009; Cheng et al., 2010). Recently, label-free aptamer biosensors have been fabricated which use either photoactive polymer or DNA-intercalating dyes to report conformational change of aptamers upon recognition of given targets (Li and Ho, 2008; Ho and Leclerc, 2004).

In contrast to the more routinely employed label technology, aptamer cross-linked hydrogel reported by Tan provided a novel method for the target detection, without the need for labeled species. In that method, gold nanoparticles (AuNPs) were trapped inside the hydrogel (Zhu et al., 2010). And simple and rapid target detection with the naked eye was developed based on the competitive binding of the target to the aptamer causing the reduction of cross-linking density and inducing gel dissolution. Because lots of signal element was encapsulated into the hydrogel this method provided a high sensitivity. As no special features on the aptamers and label progress are required, this technique provides a new generic approach that can be applied with different aptamer sequences for the detection of other molecules (Zhu et al., 2010). But the state and stability of hydrogel heavily affected by temperature, pH, ionic strength, electric field, and so on. Furthermore, the hydrogel molecular weight which affected the pore size of the hydrogel is affected by the preparation condition. Novel strategy using label free technology for detecting adenosine based on AP-site-binding ligands and engineered DNA aptamers was also reported recently (Xu et al., 2009). Herein, we fabricated a novel label-free biosensor for cancer cell detection with signal probe encapsulated by DNA.

In this work, Ramos cell was used as the model target to test our new label-free sensing method. A Ramos cell aptamer has previously been obtained by Tan's research group through an in vitro selection process (Tang et al., 2007). And Ru was selected as signal probe model. As the hybridization proceeding in the presence of Ramos cell aptamer and hybridization DNA, the three-dimensional network structure was formed and the signal probe Ru was encapsulated. Upon introduction of Ramos cell, the three-dimensional network structure was broken as a result of competitive target-aptamer binding and specific recognition between the cell and aptamer (Yang et al., 2008). And the signal probe Ru was released. With ECL detection, detection limit as low as 58 cells/mL was achieved for Ramos cell.

2. Experimental

2.1. Materials

Tris (2,2′-bipyridyl) dichlororuthenium(II) ($Ru(bpy)_3Cl_2$, abbreviated as Ru) and tripropylamine (TPA), Tris (2-carboxyethyl) phosphine hydrochloride (TCEP) were from Sigma (St. Louis, USA), 6-mercapto-1-hexanol (MCH) was purchased from Acros (Geel, Belgium). Luminol was purchased from Tokyo Chemical Industry Co. Ltd. (Tokyo, Japan). Ferrocenecarboxylic acid (FCA) was obtained from Strem Chemicals, Inc. (Newburyport, MA USA), Carboxyl groups modified magnetic nanoparticles (Carboxyl modified MBs) (1–1.5 μm, 10 mg/mL) were purchased from Baseline Chromtech Research Centre (Tianjin, China). All the reagents were analytical grade and used without further purification.

All solutions were prepared with double distilled water. The buffers involved in this work are as follows. DNA immobilization buffer: 10 mM Tris–HCl, 1.0 mM EDTA, 1.0 M NaCl, and 1.0 mM TCEP (pH 7.4); DNA hybridization buffer: 10 mM PBS, 1.0 mM EDTA, and 1.0 M NaCl (pH 6.8); Buffer for electrochemical measurements: 100 mM phosphate buffer (pH 7.4).

All synthetic oligonucleotides were purchased from SBS Genetech Co. Ltd. (Beijing, China). Their sequences were presented as follows:

Long-strand DNA: 5′-SH-CCTACCTGCATGA A CCTACCTGCATGA A CCTACCTGCATGA A CCTACCTGCATGA A CCTACCTGCATGA-3′ (containing five repeating units (underline). When MBs were used as the sensing surface SH was changed as NH_2).

Short-strand DNA, strand A: 3′-**GGATGGACGTACT** GTG GCC CTC CTA TCA AGC CA-5′ (containing complementary sequences (bold) to long-strand DNA repeating units and complementary sequences (normal) to part of aptamer (italic)).

Strand B: 3′-**GGAT GGA CGT ACT** CAC CGG GAG GAG ACC CTG AA-5′ (containing complementary sequences (bold) to long-strand DNA repeating units and complementary sequences (normal) to another part of aptamer (italic and bold));

Aptamer: 3′-*CAC CGG GAG GAT AGT TCG GT* ***G GCT GTT CAG GGT CTC CTC CCG GTG***-5′.

2.2. Apparatus

Cyclic voltammetric experiments were performed with a CHI660B Electrochemistry Working Station (CH Instruments). All experiments were carried out with a conventional three-electrode system. The working electrode was gold electrode. A Pt wire was used as the counter electrode and Ag/AgCl (sat.) was used as reference electrode, which is invariable during the experiment period. All the potentials were measured and reported according to this reference electrode. The electrogenerated chemiluminescence (ECL) intensity produced in the electrolytic cell was detected and recorded by a flow injection chemiluminescence analyzer (IFFD, Xi'an Remax Electronic Science Tech. Co. Ltd., Xi'an, China), which was operated by a personal computer.

2.3. Cell culture

Ramos cells as target cells, CEM cells and K562 as control cells were separately cultured in cell flasks according to the instructions from the American Type Culture Collection. The cell line was grown to 90% confluence in RPMI 1640 medium supplemented with 10% (v/v) fetal bovine serum (FBS) and 100 IU/mL penicillin–streptomycin at 37 °C, and the cells were cultured in a humidified atmosphere with 5% CO_2. The cell density was determined using a hemocytomer prior to each experiment. And then, a 3.0 mL suspension of $\sim 1.0 \times 10^6$ cells dispersed in RPMI 1640 cell media buffer was centrifuged at 3000 rpm for 5 min and washed with phosphate-buffered saline (18.6 mM phosphate, 4.2 mM KCl, and 154.0 mM NaCl) five times and resuspended in 1.0 mL cell media buffer.

2.4. Preparation of ECL biosensor

The procedure of the fabrication of ECL biosensor and the principle of signal probe encapsulated by DNA-based ECL detection of Ramos cell are illustrated in Scheme 1. Briefly, a gold electrode (3 mm in diameter, Jiangsu Jiangfen Electroanalytical Instrument Co., Ltd.) was polished carefully with alumina slurries (1, 0.3, 0.05 μm) and washed ultrasonically with deionized and doubly distilled water. Then it was electrochemically cleaned in 0.5 M H_2SO_4 solution by cyclic potential scanning between 0.3 and 1.5 V until a standard CV was obtained. Subsequently, the gold electrode was rinsed with deionized and doubly distilled water and absolute ethanol in turn. Then the gold electrode was dried with nitrogen gas.

Subsequently the gold electrode was immersed into 1 mL of 10 mM Tris–HCl buffer containing 1.0×10^{-7} M long-strand DNA and incubated for 5 h. In order to avoid consequent nonspecific adsorption in the following hybridization steps, the modified gold electrode was immersed in the sodium phosphate solution containing 1 mM MCH for 1 h to block the uncovered gold surface.

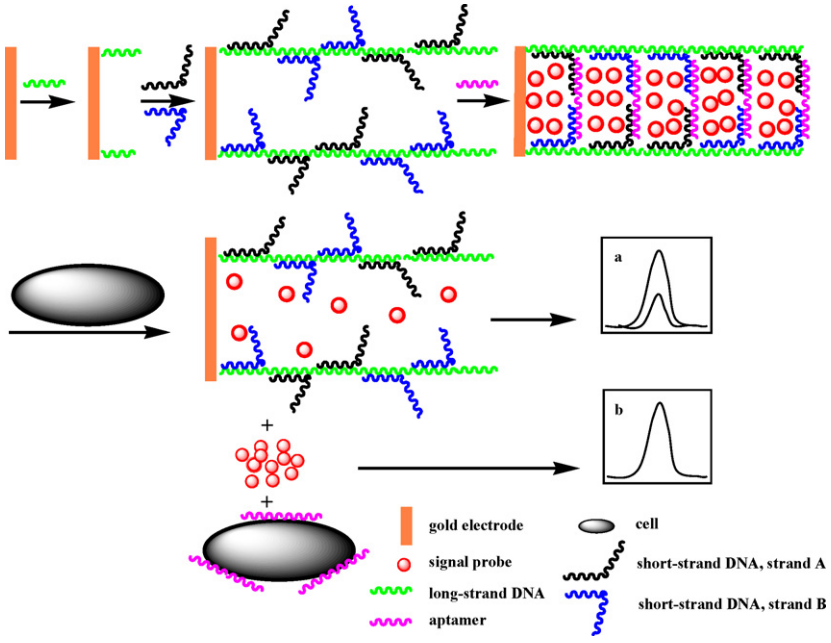

Scheme 1. Schematic diagram for the cancer cell biosensor fabrication based on encapsulating signal probe by DNA. The detection signal produced from the electrode (ECL or CC detection) (a) or the supernatant of signal probe solution (CL detection) (b).

Then, the modified electrode was immersed into 10 mM PBS buffer (pH 6.8) containing short-strand DNA, strand A and strand B at 37 °C. One hour later, the modified gold electrode was immersed into 10 mM PBS buffer containing Ru and aptamer for 12 h. Rinsing the gold electrode surface with 100 mM phosphate buffer (pH 7.4) after each step of fabrication process is very important to remove nonspecifically adsorbed sequences.

2.5. Cancer cell detection

For cancer cell assays, the prepared biosensor was immersed into 1.0 mL of cells solution of different concentrations. After incubation for 1 h at 37 °C, the gold electrode surface was washing throughout with 100 mM phosphate buffer (pH 7.4). The ECL measurement was performed in 2.0 mL of 100 mM PBS containing 100 mM TPA. As can be expected from the $Ru(bpy)_3^{2+}$-TPA ECL mechanism, the onset of luminescence occurred near 0.90 V, and then the ECL intensity rose until it reached a maximum about 1.14 V,

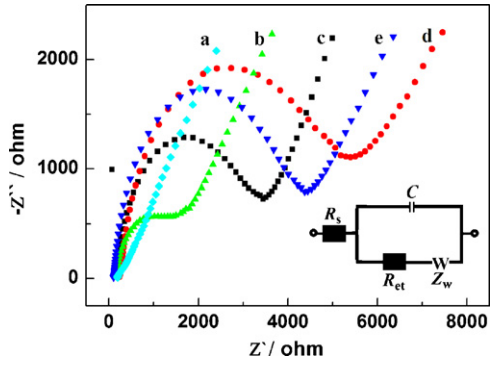

Fig. 1. Faradaic impedance spectra (Nyquist plots) corresponding to Au electrodes (a), after immobilization of long-strand DNA (b), hybridization with short-strand DNA, strand A and strand B (c), encapsulation of Ru and hybridization with aptamer simultaneous (d), and after treatment with 3000 cells/mL cancer cell (e). The data were recorded in the presence of $[Fe(CN)_6]^{3-/4-}$, 2.5 mM, as a redox label, and upon application of the biasing potential of 0.511 V, applying 5 mV alternative voltage in the frequency range of 100 mHz to 0.05 kHz. Data were recorded in a PBS solution (10 mM) that included KCl (100 mM); pH 7.4.

which was consistent with the oxidation potential of $Ru(bpy)_3^{2+}$ (at the scan rate of 100 mV/s in PBS (pH 7.2)) (Fig. S2). The concentration of cell was quantified by a decrease of ECL peak height ΔI ($\Delta I = I_0 - I$), where I_0 is the ECL peak height before the prepared biosensor incubated with the cells solution and I is the ECL peak height after incubation.

3. Results and discussion

3.1. Analytical principle of the ECL biosensor

Scheme 1 illustrates the working principle of label-free detection method. Two short-strand DNA, strand A and strand B, are grafted onto a long-strand DNA to form DNA strands A and B (L-A and L-B) through the hybridization between the long-strand DNA and strand A or strand B, respectively. The sequences of strand A and strand B are complementary to aptamer sequence. When immobilized onto the solid substrate, the L-A and L-B are in relaxed state. The addition of aptamer initiates hybridization of strand A and strand B with the aptamer sequence, thus cross-linking the L-A and L-B. As the hybridization proceeds, the four kinds of DNA will finally transform into a three-dimensional network structure (Yang et al., 2008). Upon introduction of a target object, the aptamer will bind with it, and the three-dimensional network structure of the DNA will be broken as a result of competitive target-aptamer binding (Yang et al., 2008). If a signal probe is added prior to or synchronously the addition of the aptamer, the signal probe will be trapped inside the three-dimensional network structure of the DNA (represented as red symbols in Scheme 1). When target object are introduced to interact with the three-dimensional network structure of DNA, the signal probe is released and the detection signal would decreased. And the concentration of the target object can be detected according to the detection signal produced from the electrode (ECL detection). In order to further test the fabricated method possessed generality, FCA was used as the signal probe for CC detection (named CC biosensor). And magnetic beads were used as matrix for DNA immobilization, luminol was used as signal probe for chemiluminescent (CL) detection (named CL biosensor). When the target was introduced, the Ramos cell would interact

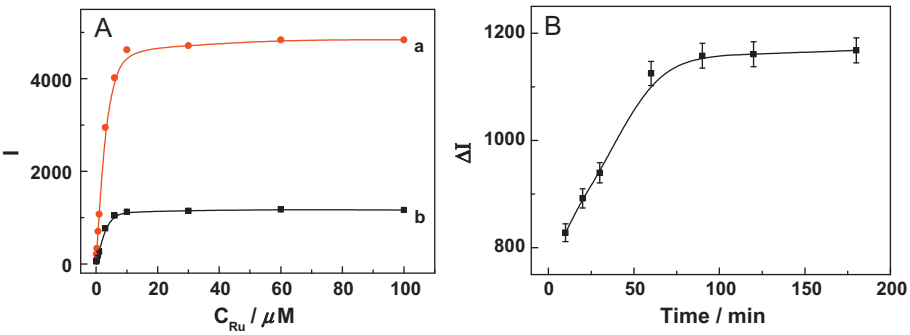

Fig. 2. (A) Effect of Ru concentration on the ECL intensity I_0 (a) and ΔI (b). (B) Effect of incubation time of the cell with biosensor on the ECL intensity (ΔI). Cell concentration is 1000 cells/mL.

with the aptamer and the FCA or luminol was released. After magnetic separation, the resulting suspension was detected with CC or CL detection. The detailed information of detection principle of CC biosensor used FCA as signal probe and CL biosensor used luminol as signal probe were described in the Supporting Information.

3.2. Characterization of the ECL biosensor

The assembly of nucleic acids on electrodes and the encapsulation of the Ru (ECL probe) and the interaction of aptamer with cancer cell were characterized by electrochemical impedance spectroscopy (EIS). The $[Fe(CN)_6]^{3-}/^{4-}$ couple as a redox probe was used in the testing solution (Patolsky et al., 1999). Fig. 1 showed a Nyquist plot of impedance for Au electrodes (Fig. 1a), after immobilization of long-strand DNA (Fig. 1b), hybridization with short-strand DNA, strand A and strand B (Fig. 1c), encapsulation of Ru and hybridization with aptamer simultaneous (Fig. 1d), and after treatment with 3000 cells/mL cancer cell (Fig. 1e). In the Nyquist plot of impedance spectra, the semicircle portion at higher frequencies corresponds to the electron-transfer-limited process and the linear portion seen at lower frequencies may be ascribed to the diffusion. The increase in the diameter of the semicircle reflects the increase in the interfacial charge-transfer resistance (R_{et}). Numerical values of R_{et} were derived from experimental impedance spectra by fitting an equivalent circuit model based on a modified Randles and Ershler model to the data. The R_{et} of the bare Au electrode was 78 Ω. After immobilization of long-strand DNA, the value of R_{et} increased to 994 Ω. The increase in R_{et} is due to the immobilization of negatively charged DNA on the electrode surface resulting in a negatively charged interface that electrostatically repels the negatively charged redox probe $[Fe(CN)_6]^{3-}/^{4-}$ and inhibits interfacial charge-transfer (Cho et al., 2006). After hybridization with short-strand DNA, the value of R_{et} was increased to 2470 Ω, due to the large amount of DNA linked on Au electrode. After encapsulation of Ru and hybridization with aptamer simultaneous, the interfacial electron resistance increased to 4020 Ω. This indicates that Ru is encapsulated onto network of the electrode and more DNA was linked on Au electrode. When the fabricated biosensor was immersed in cell solution (3000 cells/mL), the R_{et} decreased 35.82% from 4020 Ω to 2580 Ω (curve e). This is attributed to the fact that the bound aptamer is forced to dissociate from the surface of electrode due to the formation of the aptamer–cell complex and part of Ru is also dissociated from the surface of electrode at the same time.

3.3. Stability of the ECL biosensor

Stability is also an extremely important feature for biosensors in the practical applications such as clinical diagnoses. The long-term storage stability of this ECL biosensor kept in 10 mM phosphate buffer solution at 4 °C was concerned. The experimental results suggested that this biosensor is fairly robust. After biosensor preparation, gold electrodes with DNA and Ru could be stored in the refrigerator with minimal loss of DNA and Ru for at least 24 h. After storage 24 h, ECL intensity (I_0) of the biosensor almost retained 98.1% intensity of the original performance and decreased ECL intensity (ΔI) after this biosensor performance using 1000 cells/mL also retained 97.4% intensity of the original performance. The long-term storage stability of the ECL sensor immerged in solution at room temperature was also studied. The cyclic voltammetry measurements were also performed by monitoring ECL intensity of this sensor immerged in 0.1 M PBS (pH 7.4) every 2 h. The ECL intensity only decreased 2.2% compared with the initial steady state value after 6 h of immersion in PBS solution.

The same experimental results were obtained when FCA was used as the signal probe and magnetic beads were used as matrix for DNA immobilization, luminol was used as signal probe for CL detection. CC intensity of FCA decreased only 3.2% after the CC biosensor storage 24 h in solution at 4 °C. The decreased CC intensity after CC biosensor performance using 1000 cells/mL also retained 97.0% intensity of the original performance. The CC intensity decreased 3.1% after 6 h of immersion in PBS solution. There is no obvious detected CL intensity of supernatant of MBs solution after CL biosensor immerged in 0.1 M PBS (pH 7.4) for about 6 h. The results suggested that Ru, FCA and luminol molecules were well encapsulated in the DNA network (the details information about the encapsulation of the signal element can be found in ESI). Because the DNA network is relatively steady frame at certain condition (Liu et al., 2005), Ru, FCA and luminol molecules can be stably encapsulated in the DNA network. This would lead to the good stability of this biosensor.

3.4. Effect of encapsulation mode for ECL

The different modes of signal probe encapsulation greatly affected the ECL intensity. The encapsulation of signal probe were first comprehensively analysed by three different addition sequence of signal probe (the three modes can been seen in supporting information). The experimental results suggested that the maximum signal intensity can be obtained when mode C was used. In this mode signal probe was first added into the short-strand DNA solution for encapsulation. After washing the matrix, signal probe was again added into the aptamer solution for encapsulation. From the ECL intensity (I_0) it can be concluded that maximum dose of signal probe was encapsulated into the three-dimensional network structure of DNA compared with that of the other two modes (mode A and mode B). But it was also found that mode B gives the relative stronger ECL intensity. The ECL intensity from mode B is 97.6% of that from mode C. However, ECL intensity from the mode A only is 8.9% of that from mode C. The experimental results show that the general trends of FCA and luminol being used

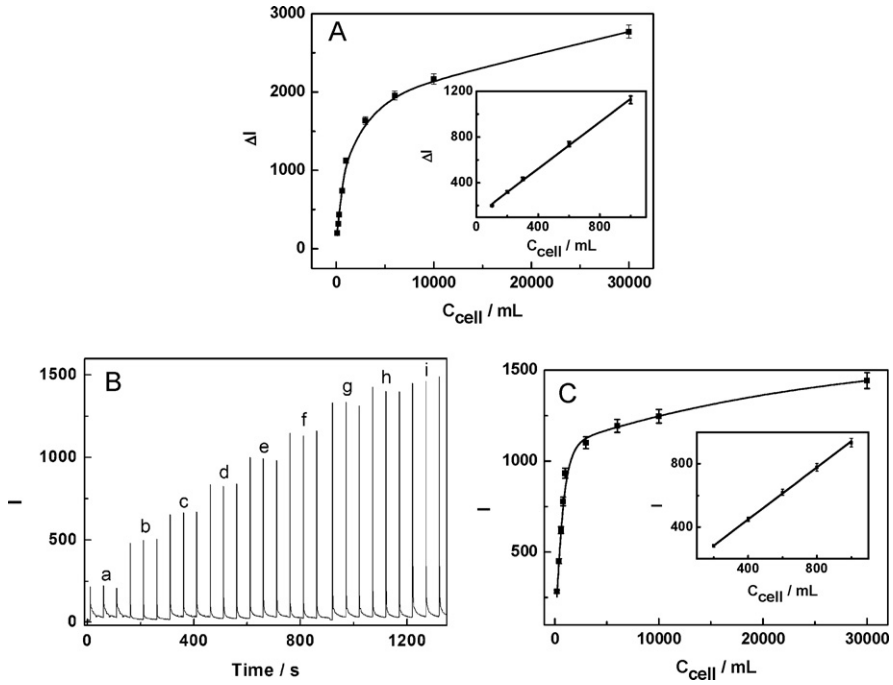

Fig. 3. (A) The calibration curve of ECL versus the concentration of Ramos cell from 100 to 30,000 cells/mL. Inset is the amplification of the linear range from 100 to 1000 cells/mL for Ramos cell determination. (B) The CL response of different concentrations of Ramos cell of (a) 0, (b) 200, (c) 300, (d) 600, (e) 1000, (f) 3000, (g) 6000, (h) 10,000, (i) 30,000 cells/mL. (C) The calibration curve of CL versus the concentration of Ramos cell from 200 to 30,000 cells/mL. Inset is the amplification of the linear range from 200 to 1000 cells/mL for Ramos cell determination.

as signal probe are similar. Considering there is no essentially difference of ECL intensity of mode B from mode C and simplify of mode B, we adopted mode B for the following experiments. It was also confirmed that the signal probe was physically trapped into the three-dimensional network structure of the DNA rather than the intercalation binding between signal probe and DNA. In order to validate the encapsulation of signal probe is mediated by aptamer, mutant aptamer (arbitrary sequence) was used as substitute for aptamer. There is nearly no ECL response. It confirmed that the hybridization between the aptamer and L-A and L-B results in the encapsulation of signal probe.

3.5. Optimization of the experimental conditions

In order to get the optimal analytical parameters, the relative experiment conditions such as incubation time of the cell with biosensor, concentration of Ru in encapsulation solution was investigated.

The Ru concentration in the encapsulation solution was firstly optimized with the ECL intensity. In order to investigate the effect Ru concentration on the ECL intensity, the biosensor was performed using 1000 cells/mL Ramos cells. We observed that I_0 was enhanced significantly when the Ru concentration increased from 0.1, 0.3, 0.6, 1.0, 3.0, 6.0 to 10.0 μmol/L. And the ΔI also increased greatly. However, at concentrations >10 μmol/L I_0 was enhanced slowly and ΔI became more flattened. This was attributed to the fact that more Ru molecule was encapsulated into the DNA network on the surface of electrode when Ru concentration increased from 0.1 to 10 μmol/L. But at Ru concentration >10 μmol/L, the Ru molecule on the surface of electrode was tended to saturated so the I_0 was enhanced slowly and ΔI became more flattened. So 10 μmol/mL Ru was used for further investigation.

Since concentration of cell and reaction time are closely related, the concentration of cell was fixed at 1000 cells/mL when we investigated the effect of incubation time of the cell with biosensor on ECL intensity. Fig. 2B shows the effect of the incubation time of the cell with biosensor on ECL intensity. Because the interaction between cell and aptamer is a fast binding process, the ΔI would increase with the increasing incubation time (Kang et al., 2010). As expected, ECL intensity obviously decreases with increasing the incubation time from 10 min to 30 min and then reaches a plateau in 60 min (Fig. 2B). After 60 min, ECL intensity decreased very slowly. ΔI changed oppositely and it increased with increasing the incubation time from 10 min to 30 min and then also reaches a plateau in 60 min. Further incubation was not capable of leading to the obvious ECL response change and ΔI increased very slowly. This can be explained by the passive absorption between aptamer and target cells. The longer incubation time will introduce more events of this nonspecific interaction between aptamer and cells. As the aim was to optimize an assay to be both as quick and as efficient as possible, it was decided to perform 1-h incubations in further experiments.

3.6. ECL response of the biosensors to the cancer cell

When the target was introduced, the Ramos cell would interact with the aptamer and the Ru was released. The amount of the Ru on the surface of electrode would decrease. Because of the high sensitivity of ECL detection and a mass of Ru encapsulated, a few Ramos cells would lead to many Ru molecule being released and give rise to obvious detectable signal. The quantitative behavior of the ECL biosensors was assessed by measuring the dependence of the decreased ECL intensity (ΔI) upon the concentration of Ramos cell. Under the optimized test conditions, the linear range and detection limit of biosensors to the Ramos cell were measured. The results showed that the decreased ECL intensity (ΔI) of the biosensor was exponentially related to the concentration of Ramos cell in the range from 100 to 30,000 cells/mL. The regression equation was $\Delta I = -1561.76 \times \exp(-C/15{,}525.73) - 1417.88 \times \exp(-C/882.61) + 2995.54$ with a regression coefficient of 0.9991. The linear range for cancer cell was 100–1000 cells/mL with the equation of $\Delta I = 1.02\,C + 114.77$ (ΔI is the decreased ECL intensity; C is the concentration of cancer cell; $n = 5$, $R^2 = 0.9994$) and the detection limit

Table 1
Comparison between the current method and other reported techniques for analysis of Ramos cell.

Assay format[a]	Detection system[b]	Detection range[c]	Detection limit[c]	Reference
Circular strand -displacement polymerization	Flu	Ramos: 1×10^2–1×10^4	100	Ding et al. (2010)
Direct	Col	CEM: 6.6×10^2–1.3×10^5	300	Medley et al. (2008)
ACNPs	Flu	CEM: 5×10^3–2×10^5	1250	Smith et al. (2007)
Enzyme-linked	DPV	K562: 5×10^4–1×10^7	1.0×10^4	Du et al. (2005)
Electrodeposition	Imp	K562: 5×10^3–5×10^7	1.0×10^3	Hao et al. (2007)
Cytosensor	DPV	BGC: 1×10^3–1×10^7	620	Cheng et al. (2008)
Self-assembled monolayer	ASV	K562: 1×10^2–1×10^7	-[d]	Ding et al. (2008)
Ferrocene-concanavalin alectin-probe	CV	K562: 1×10^4–1×10^7	1.0×10^3	Xue et al. (2010)
Carbohydrate-functionalized CdS nanocomposite	ECL	BGC: 2×10^3–1×10^7	1.2×10^3	Han et al. (2010)
Signal probe encapsulated by DNA	ECL	Ramos: 1×10^2–3×10^4	58	
Signal probe encapsulated by DNA	CL	Ramos: 2×10^2–3×10^4	126	[e]
Signal probe encapsulated by DNA	CC	Ramos: 2×10^2–3×10^4	78	

[a] ACNPs: aptamer-conjugated nanoparticles; ACMNPs: aptamer-conjugated magnetic nanoparticles.
[b] DPV: differential pulse voltammetry. ASV: anodic stripping voltammetric; CL: chemiluminescence; ECL: electrogenerated chemiluminescence; CC: chronocoulometry; Flu: fluorescence; Imp: impedance; Col: colorimetric; CV: cyclic voltammetric
[c] In cells/mL.
[d] Do not reported in their paper.
[e] This method.

of 58 cells/mL estimated using 3σ (Fig. 3). A series of seven repetitive measurements of 1000 cells/mL were used for estimating the precision, and the relative standard deviation (RSD) was 3.2%. It was shown that this ECL biosensor had good reproducibility. This method and some other amplified techniques, which can greatly improve the sensitivity of the Ramos cell assay, are listed in Table 1. Comparing to other methods based on amplification technology listed in Table 1, the current protocol is one of the most sensitive assay for the determination of Ramos cells.

The sensitivity of this work was found to be increased about 1–4 orders of magnitude than that of some methods (Medley et al., 2008; Smith et al., 2007; Du et al., 2005) and it is even more sensitive than the most sensitive work reported by Ding's using fluorescence detection (Ding et al., 2010). Because the biosensor could be prepared before the detection experiment the total detection time of this method is about 1 h, which was competitive compared to the methods with a similar detection limit. Only need a signal probe and some DNA, the direct detection of Ramos cell could be accomplished with one step, so the low cost and simple operation was another merit compared to other methods.

The linear range and detection limit of biosensors to the Ramos cell were measured when luminol was used as the signal probe. As shown in Fig. 3B, for the CL biosensor, the CL signal increased with the increase of the concentration of Ramos cell, and the CL intensity revealed an exponential relationship with the concentration of Ramos cell ranging from 200 to 30,000 cells/mL. The linear range for Ramos cell was 200–1000 cells/mL with the equation of $I = 0.814\,C + 124.4$ ($n = 5$, $R^2 = 0.9996$). A detection limit of 126 cells/mL Ramos cell can be estimated using 3σ for CL biosensor and EC biosensor (3σ). And the CC biosensor gives an exponential relationship with the concentration of Ramos cell ranging from 100 to 30,000 cells/mL. The linear range for Ramos cell was 100–1000 cells/mL with detection limit of 76 cells/mL Ramos cell. The equation is $I = 0.0026\,C - 0.1902$ ($n = 7$, $R^2 = 0.9986$).

3.7. Selectivity of the cancer cell biosensor

In order to evaluate the selectivity, the biosensor was performed using Ramos cells, CEM cells, K562 cells and artificial complex samples by mixing equal amounts of Ramos cells and CEM cells, Ramos cells and K562 cells respectively. As shown in Fig. 4, a well-defined ΔI was obtained for Ramos cells. ΔI for artificial complex samples was almost the same as that for Ramos cells at the same concentration, and CEM cells and K562 cells showed nearly no response. It proved that this biosensor has an excellent capability in discriminating target cancer cell from the non-target cancer cell. The selectivity of this biosensor was due to the affinity of aptamer to Ramos cell (Huang et al., 2009a,b).

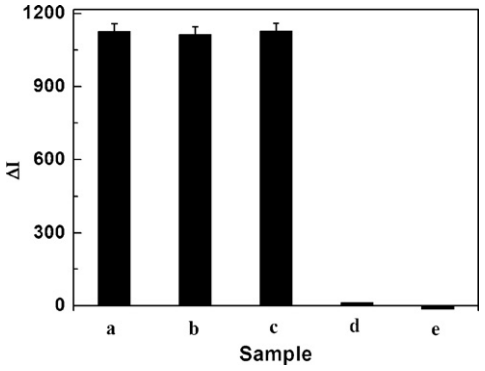

Fig. 4. ECL responses for different cells. (a) Ramos cells; (d) CEM cells; (e) K562 cells; (b) artificial complex containing equal amounts of Ramos cells and CEM cells; (c) artificial complex containing equal amounts of Ramos cells and K562 cells. The concentrations were 1000 cells/mL for (a), (d) and (e); artificial complex (b) and (c) containing 1000 cells/mL Ramos cells, CEM cells and K562 cells respectively. The blank was deducted.

4. Conclusions

We report a novel approach to Ramos cancer cell detection via label-free biosensor using signal probe encapsulated by DNA exhibiting very high sensitivity and selectivity. These features, as well as its operation convenience, and stability, make it a promising alternative to conventional cancer detection methods. Under the conditions of 60 min of incubation time, aptamer-DNA conjugates can specifically bind with target cells and release the loaded signal probe. Since the fabricated biosensor is ECL, CL or CC-based, one might expect the design of an integrated, portable, and low-cost device for cancer detection based on the proof-of-concept approach described in this work.

Acknowledgements

This research was supported by the National Natural Science Foundation of China (21005045), the Scientific and Technical Development Project of Qingdao (09-1-3-45-jch), the Scientific Research Startup Foundation of Qingdao University of Science and Technology for Talents, the Excellent Young Scientists Founda-

tion of Shandong Province (No. JQ200805) and the National Basic Research Program of China (No. 2010CB732404).

Appendix A. Supplementary data

Supplementary data associated with this article can be found, in the online version, at doi:10.1016/j.bios.2011.03.004.

References

Cerchia, L., Hamm, J., Libri, D., Tavitian, B., de Franciscis, V., 2002. FEBS Lett. 528, 12.
Cheng, W., Ding, L., Lei, J., Ding, S., Ju, H., 2008. Anal. Chem. 80, 3867.
Cheng, W., Chen, Y.L., Yan, F., Ju, H.X., Yin, Y.B., 2010. Chem. Commun. 46, 6720.
Cho, M., Lee, S., Han, S.Y., Park, J.Y., Rahmen, M.A., Shim, Y.B., Ban, C., 2006. Nucleic Acids Res. 34, 75.
Ding, C.F., Li, X.L., Ge, Y., Zhang, S.S., 2010. Anal. Chem. 82, 2850.
Ding, L., Cheng, W., Wang, X.J., Ding, S.J., Ju, H.X., 2008. J. Am. Chem. Soc. 130, 7224.
Du, D., Ju, H.X., Zhang, X.J., Chen, J., Cai, J., Chen, H.Y., 2005. Biochemistry 44, 11539.
Espina, V., Geho, D., Mehta, A.I., Petricoin III, E.F., Liotta, L.A., Rosenblatt, K.P., 2005. Cancer Invest. 23, 36.
Famulok, M., Hartig, J.S., Mayer, G., 2007. Chem. Rev. 107, 3715.
Han, E., Ding, L., Jin, S., Ju, H.X., 2010. Biosens. Bioelectron. 26, 2500.
Hao, C., Ding, L., Zhang, X., Ju, H., 2007. Anal. Chem. 79, 4442.
Ho, H.A., Leclerc, M., 2004. J. Am. Chem. Soc. 126, 1384.
Huang, Y.F., Lin, Y.W., Lin, Z.H., Chang, H.T., 2009a. J. Nanopart. Res. 11, 775.
Huang, Y.F., Shangguan, D.H., Liu, H.P., Phillips, J.A., Zhang, X.L., Chen, Y., Tan, W.H., 2009b. ChemBioChem 10, 862.
Hun, X., Zhang, Z.J., Tiao, L., 2008. Anal. Chim. Acta 625, 201.
Jayasena, S.D., 1999. Clin. Chem. 45, 1628.
Kang, H.Z., O'Donoghue, M.B., Liu, H.P., Tan, W.H., 2010. Chem. Commun. 46, 249.
Layzer, J.M., Sullenger, B.A., 2007. Oligonucleotides 17, 1.
Li, N., Ho, C.M., 2008. J. Am. Chem. Soc. 130, 2380.
Liu, X., Ma, L., Cheng, C., Wang, Y., Miyajima, H., Zhao, Y., 2005. Nucleosides Nucleotides Nucl. Acids 24, 199.
Mayer, G., Raddatz, M.S., Grunwald, J.D., Famulok, M., 2007. Angew. Chem. Int. Ed. 46, 557.
Medley, C.D., Smith, J.E., Tang, Z.W., Wu, Y.R., Bamrungsap, S., Tan, W.H., 2008. Anal. Chem. 80, 1067.
Murray, A., Chapman, C.J., Healey, G., Peek, L.J., Parsons, G., Baldwin, D., Barnes, A., Sewell, H.F., Fritsche, H.A., Robertson, J.F.R., 2010. Ann. Oncol., mdp 606v1.
Patolsky, F., Zayats, M., Katz, B., Willner, I., 1999. Anal. Chem. 71, 3171.
Shangguan, D.H., Li, Y., Tang, Z.W., Cao, Z.H.C., Chen, H.W., Mallikaratchy, P., Sefah, K., Yang, C.Y.J., Tan, W.H., 2006. Proc. Natl. Acad. Sci. U.S.A. 103, 11838.
Shangguan, D.H., Tang, Z.W., Mallikaratchy, P., Xiao, Z.Y., Tan, W.H., 2007. ChemBioChem 8, 603.
Smith, J.E., Medley, C.D., Tang, Z., Shangguan, D.H., Lofton, C., Tan, W.H., 2007. Anal. Chem. 79, 3075.
Tang, Z.W., Shangguan, D.H., Wang, K.M., Shi, H., Sefah, K., Mallikaratchy, P., Chen, H.W., Li, Y., Tan, W.H., 2007. Anal. Chem. 79, 4900.
Xu, Z.A., Sato, Y., Nishizawa, S., Teramae, N., 2009. Chem. Eur. J. 15, 10375.
Xue, Y.Y., Ding, L., Lei, J.P., Ju, H.X., 2010. Biosens. Bioelectron. 26, 169.
Yang, C.J., Jockusch, S., Vicens, M., Turro, N., Tan, W.H., 2005. Proc. Natl. Acad. Sci. U.S.A. 102, 17278.
Yang, H.H., Liu, H.P., Kang, H.Z., Tan, W.H., 2008. J. Am. Chem. Soc. 130, 6320.
Zheng, D., Seferos, D.S., Giljohann, D.A., Patel, P.C., Mirkin, C.A., 2009. Nano Lett. 9, 3258.
Zhu, Z., Wu, C.C., Liu, H.P., Zou, Y., Zhang, X.L., Kang, H.Z., Yang, C.Y.J., Tan, W.H., 2010. Angew. Chem. Int. Ed. 49, 1052.